MOLECULAR AND CELLULAR BIOLOGY, Dec. 2007, p. 8783–8796 Vol. 27, No. 24
0270-7306/07/$08.00+0 doi:10.1128/MCB.01204-07

Initiation of Protein O Glycosylation by the Polypeptide GalNAcT-1 in Vascular Biology and Humoral Immunity▽†

Mari Tenno,[1] Kazuaki Ohtsubo,[1] Fred K. Hagen,[2] David Ditto,[3] Alexander Zarbock,[4] Patrick Schaerli,[5] Ulrich H. von Andrian,[5] Klaus Ley,[6] Dzung Le,[3] Lawrence A. Tabak,[7] and Jamey D. Marth[1]*

Howard Hughes Medical Institute and Department of Cellular and Molecular Medicine, University of California San Diego, La Jolla, California[1]; Department of Biochemistry and Biophysics, University of Rochester, School of Medicine and Dentistry, Rochester, New York[2]; Department of Pathology, University of California San Diego, La Jolla, California[3]; Department of Anesthesiology and Critical Care Medicine, University of Muenster, Muenster, Germany[4]; CBR Institute for Biomedical Research and Department of Pathology, Harvard Medical School, Boston, Massachusetts[5]; Cardiovascular Research Center and Department of Biomedical Engineering, University of Virginia, Charlottesville, Virginia[6]; and Section on Biological Chemistry, National Institute of Diabetes and Digestive and Kidney Diseases, National Institutes of Health, Department of Health and Human Services, Bethesda, Maryland[7]

Received 6 July 2007/Returned for modification 18 September 2007/Accepted 25 September 2007

Core-type protein O glycosylation is initiated by polypeptide *N*-acetylgalactosamine (GalNAc) transferase (ppGalNAcT) activity and produces the covalent linkage of serine and threonine residues of proteins. More than a dozen ppGalNAcTs operate within multicellular organisms, and they differ with respect to expression patterns and substrate selectivity. These distinctive features imply that each ppGalNAcT may differentially modulate regulatory processes in animal development, physiology, and perhaps disease. We found that ppGal NAcT-1 plays key roles in cell and glycoprotein selective functions that modulate the hematopoietic system. Loss of ppGalNAcT-1 activity in the mouse results in a bleeding disorder which tracks with reduced plasma levels of blood coagulation factors V, VII, VIII, IX, X, and XII. ppGalNAcT-1 further supports leukocyte trafficking and residency in normal homeostatic physiology as well as during inflammatory responses, in part by providing a scaffold for the synthesis of selectin ligands expressed by neutrophils and endothelial cells of peripheral lymph nodes. Animals lacking ppGalNAcT-1 are also markedly impaired in immunoglobulin G production, coincident with increased germinal center B-cell apoptosis and reduced levels of plasma B cells. These findings reveal that the initiation of protein O glycosylation by ppGal NAcT-1 provides a distinctive repertoire of advantageous functions that support vascular responses and humoral immunity.

A large fraction of cellular protein O glycosylation is directed to producing a series of core-type O-glycan structures that begin with the covalent linkage of *N*-acetylgalactosamine (GalNAc) to serine and threonine residues of proteins in the secretory pathway (10, 35, 38, 58, 61). This initial enzymatic step by a polypeptide GalNAc transferase (ppGalNAcT) is followed in the Golgi apparatus by the regulated attachment of other saccharide linkages to this GalNAc residue by other glycosyltransferases, contributing to the changing O-glycan repertoire of a given cell (8, 45). Full disclosure of ppGalNAcT structure and expression was made possible by biochemical purification of the enzymatic activity, followed by acquisition of the amino acid sequence (17, 24). Unexpectedly, multiple cDNAs encoding apparent ppGalNAcT isozymes were discovered, while genetic disruption of ppGalNAcT in the mouse failed to ablate O-glycan formation in vivo (19, 22, 34, 48, 53, 63, 68). A large family of ppGalNAcTs is now evident among multicellular organisms analyzed thus far, with mammals expressing at least 15 ppGalNAcT isozymes encoded by different genes (9, 55).

The prototypic ppGalNAcT family member is ppGal NAcT-1, which is expressed at high levels and is found broadly among most tissues and cell types (17, 24, 30, 66). ppGal NAcT-1 exhibits a selective preference for some polypeptide sequences (7, 16, 60), further suggesting that a key function is likely provided by its activity among cells of intact organisms. The ppGalNAcT family of glycosyltransferases initiates core-type O-glycan formation, primarily consisting of core 1, core 2, core 3, and core 4 O-glycan subtypes that may be elaborated further by glycan linkages, contributing to selectin ligand-dependent control of leukocyte trafficking, regulation of $CD8^+$ T-cell apoptosis, and sensitivity to colitis and preventing the onset of Tn syndrome (11, 27, 42, 59, 65). Other endogenous functions have been established among invertebrate model organisms bearing diminished levels of various core-type O-glycans (1, 46, 54, 56).

Comparative analysis of ppGalNAcT members further indicates that not all are created equal. Besides considerable differences in tissue and cell type expression patterns, substrate specificities among polypeptides of ppGalNAcT isozymes are also significantly varied (30, 36, 40, 66). Preferences for dissimilar polypeptide sequences have been observed along with the existence of a hierarchical process in protein O glycosylation that reflects the influence of adjacent core-type O-glycan

* Corresponding author. Mailing address: Howard Hughes Medical Institute, University of California San Diego, 9500 Gilman Drive, MC0625, La Jolla, CA 92093. Phone: (858) 534-6526. Fax: (858) 534-6724. E-mail: jmarth@ucsd.edu.

† Supplemental material for this article may be found at http://mcb.asm.org/.

▽ Published ahead of print on 8 October 2007.

linkages in substrate recognition by some ppGalNAcTs (5, 20, 28, 53). These findings together indicate that functional redundancy among ppGalNAcTs is likely limited and that each may provide key physiologic roles in vertebrates, reflecting the significant level of orthologous ppGalNAcT gene sequence conservation throughout speciation. Thus far, however, mammalian models of ppGalNAcT deficiency, including ppGalNAcT-4, -5, and -13 deficiencies, lack obvious physiologic manifestations linked with decreased O-glycan formation and indicative of vital endogenous roles (22, 55, 68). Further investigations are warranted, however, and mutations in the human *GALNT3* gene, encoding ppGalNAcT-3, have been described for familial tumoral calcinosis, likely reflecting reduced protein O glycosylation (4, 26, 29, 57). Discovering biologically relevant roles of ppGalNAcTs by using intact model organisms should ultimately reveal why natural selection has maintained this family of glycosyltransferases during the evolution of multicellular organisms.

In order to detect physiologic activities linked to ppGal NAcT-1 in a mammalian model system, we generated and characterized intact mice lacking ppGalNAcT-1. We found that although ppGalNAcT-1 deficiency is generally tolerated and does not cause infertility, substantial defects occur in the formation of selectin ligands, resulting in altered innate and adaptive immune cell trafficking. In addition, ppGalNAcT-1 supports O-glycoprotein expression among a subset of blood coagulation factors, such that its deficiency results in a moderate to severe bleeding disorder. A key role of ppGalNAcT-1 in promoting adaptive immunity is also evident by an increase in germinal center (GC) B-cell apoptosis, leading to reduced plasma B-cell numbers and a substantial reduction in immunoglobulin G (IgG) antibody isotype abundance. These phenotypic and mechanistic findings indicate that distinctive physiologic activities are controlled by ppGalNAcT-1 in comparison with other similarly studied glycosyltransferase deficiency states and establish evidence of advantageous biologic purpose linked to the maintenance of ppGalNAcT-1 within the mammalian genome.

MATERIALS AND METHODS

ppGalNAcT-1 gene mutagenesis. Isolation of mouse ppGalNAcT-1 genomic DNA and construction of a targeting vector bearing Cre/loxP recombinant signals were accomplished using a human cDNA probe according to previously described procedures (41). Mice bearing the loxP-flanked exon 3 were bred with Zp3-Cre transgenic mates, as described previously (47). Genotyping was performed using Southern blotting and PCR according to previously published procedures (41). The wild-type ppGalNAcT-1 allele was detected as a 300-bp fragment by using primers P1 (5′-TCATCACAGTGTCTACCATGGCTG GAG) and P3 (5′-GATCTGATGACCTGTTGTGGACACCTG), while the targeted *F*[*tkneo*] allele was detected using P1 and P2 (5′-TTCCAGGACAGCCA GGGCTACACAGAG), yielding a 550-bp fragment.

ppGalNAcT enzyme activity. Tissues were extracted and analyzed as described previously (18). Enzyme assays for ppGalNAcT-1 activity were performed at 37°C for 1 to 2 h, using the peptide acceptor PRFQDSSSKAPPPLPSPSRLPG in a final volume of 25 μl containing 50 μM UDP-GalNAc (77,000 cpm ^{14}C), 5 mM AMP, 10 mM $MnCl_2$, 40 mM cacodylate, pH 6.5, 40 mM β-mercaptoethanol, and 0.1% Triton X-100. Products were characterized by anion-exchange chromatography and evaluated by reverse-phase high-performance liquid chromatography.

Subcloning and expression of ppGalNAcT-1 cDNAs. Isolation of cDNAs from wild-type and ppGalNAcT-1 exon 3 deletion mice was achieved by reverse transcription-PCR amplification, using mouse kidney total RNA reverse transcribed with a first-strand cDNA synthesis kit (Clontech). The luminal region of ppGalNAcT-1 was amplified using the PCR primers Mlu-mT1 (5′CACACGCG TTGCCTGCTGGTGACGTTCTAGAGCTAGT) and Bam-mT1 (5′ATGCGG ATCCAGCCCAGTCAATCCTTCCTT) to incorporate an MluI cloning site into the stem region of mouse ppGalNAcT-1. This MluI-BamHI cDNA fragment was cloned into the MluI-BamHI sites of the mammalian expression vehicle pIMKF3. Three independent ppGalNAcT-I cDNA clones bearing wild-type and deletion alleles were isolated and characterized. The DNA sequence was acquired for all clones. Expression of the recombinant enzymes was achieved by transient transfection of COS7 cells, using Lipofectamine (Life Technologies). All six constructs were transfected in duplicate. Enzyme assays for ppGalNAcT activity were performed at 37°C under standard assay conditions, with a final reaction volume of 25 μl containing 500 μM EA2 peptide (PTTDSTTPAPTTK), 50 μM UDP-GalNAc (20,000 cpm ^{14}C), 10 mM $MnCl_2$, 40 mM cacodylate, pH 6.5, 40 mM β-mercaptoethanol, and 0.1% Triton X-100.

Bleeding time. Mice were anesthetized by a mixture of 3% isoflurane with oxygen in an induction chamber and then maintained with a nose cone in a warm brass cone restraint. Tails of horizontally restrained mice were transected 2 mm from the tip with a new razor blade and then immersed vertically ~2 cm below the surface of 37°C saline. The time until bleeding stopped for at least 10 seconds was recorded. If the bleeding continued at 10 min, the tail was withdrawn from saline and the tip cauterized to stop bleeding.

Hematology. Mice were anesthetized by a mixture of 3% isoflurane with oxygen in an induction chamber and maintained with a nose cone outside the induction chamber. Tails of mice were transected 2 mm from the tip with a new razor blade. One hundred microliters of blood was allowed to drip into EDTA-containing polypropylene microtubes (Becton Dickinson, NJ). Blood in tubes was immediately mixed well to ensure proper anticoagulation and kept at room temperature until analysis (within 4 hours). Blood cell counts with leukocyte differential and platelet counts were performed in duplicate on a Hemavet 850FS multispecies hematology system (Drew Scientific, CT) programmed with mouse hematology settings. A whole blood smear was prepared from each sample and Wright stained for manual viewing.

Serum chemistry. Blood was collected from anesthetized mice as described for hematology, but without EDTA. Blood was allowed to clot for 3 to 5 h at room temperature and centrifuged in a serum separator tube for 5 min at 7,000 × *g*. Serum was removed and analyzed with a Beckman CX-7 automated chemistry analyzer.

Coagulation. Up to 1 ml of blood was quickly withdrawn from the heart of a mouse anesthetized as described for hematology, using a 1-ml plastic syringe with a 25-gauge needle containing 30 μl buffered citrate (0.06 ml/liter sodium citrate plus 0.04 ml/liter citric acid). Blood was added to a plastic tube containing sufficient additional citrate to achieve a final ratio of 9 parts whole blood to 1 part citrate. Blood was immediately mixed well and centrifuged twice at 2,000 relative centrifugal force for 15 min to obtain citrated platelet-poor plasma. Plasma samples were aliquoted and frozen at −80°C until being processed for coagulation analysis. von Willebrand factor (VWF) analysis was performed as described previously (12). Factor VIII and other factors were analyzed as described elsewhere (62).

Flow cytometry. Single-cell suspensions from the spleen, thymus, lymph nodes, and bone marrow were prepared, and red blood cells were removed by ammonium chloride lysis. Antibodies to CD3 (2C11), CD8 (53-6.7), CD40 (HM40-3), CD62L (MEL-14), B7.2 (GL1), and Gr1 (RB6-8C5) were purchased from eBioscience. Antibodies to CD4 (RM4-5), CD11a (2D7), CD11b (M1/70), CD18 (C71/16), CD19 (1D3), CD24 (M1/69), CD44 (IM7), CD45R/B220 (RA3-6B2), activated caspase-3, Fas/CD95, GL7, IgM (R6-60.2), IgG1 (A85-1), IgG2a/2b (R2-40), IgG3 (R40-82), I-A^b (AF6-120.1), and P-selectin glycoprotein ligand 1 (PSGL-1) (2PH1) were acquired from Pharmingen. Cells were incubated in the presence of various antibodies (above) in fluorescence-activated cell sorter buffer (2% fetal calf serum [FCS] in phosphate-buffered saline [PBS]) for 20 min at 4°C. For E- or P-selectin binding, cells were treated with 0.5 μg/ml of Fc block (anti-CD32/16; Pharmingen) and then incubated with anti-Gr1 antibody as described previously, with and without the addition of 5 mM EDTA for 30 min (33). Cells were washed and incubated with a goat anti-human fluorescein isothiocyanate (FITC)-conjugated secondary antibody (Sigma). Peanut agglutinin (PNA) lectin (Vector) binding was accomplished as previously described (59). Activated caspase-3 analysis by cytometry was done by permeabilizing cells using BD Cytofix/Cytoperm solution for 20 min at 4°C, followed by washing cells twice with PermWash solution (Pharmingen). Data were analyzed on a FACSCalibur flow cytometer using Cellquest software (Becton Dickinson).

Histology. Frozen sections of lymph nodes or spleen were cut at 5 μm, air dried, fixed in acetone, and incubated with biotinylated anti-CD4, biotinylated anti-CD8, anti-CD45R/B220, anti-GL7, anti-activated caspase-3, anti-FDC-M1 (Pharmingen), anti-CD68 (Serotec), and PNA. After being washing, sections were incubated with streptavidin-FITC and goat anti-rat rhodamine-conjugated secondary antibody. For L-selectin binding, sections were incubated with an L-selectin–IgG chimera and with MECA-79 antibody and then incubated with

goat anti-human IgG FITC-conjugated secondary antibody and goat anti-rat rhodamine-conjugated secondary antibody. DNA fragmentation was measured by terminal deoxynucleotidyltransferase-mediated dUTP-biotin nick end labeling (TUNEL) assay (Promega) according to the manufacturer's instructions. The mean fluorescence was analyzed using a MetaMorph system (Universal Imaging Corporation).

Lymphocyte trafficking. Homing assays were carried out with 2.5×10^7 cells isolated and incubated with the CellTracker probe CMFDA (Molecular Bioprobes) prior to injection into the tail vein as previously described (33). Lymphoid organs were harvested 1 h or 24 h after injection, and T and B lymphocytes positive for CMFDA were measured by flow cytometry.

Perfused microflow chamber. We used microflow chambers as previously described (67). Briefly, microflow chambers were constructed from 20- by 200-μm rectangular glass capillaries with a length of 30 mm (VitroCom, Mountain Lake, NJ). The capillary was placed between two microscope coverslips, and the ends were attached to heparinized polyethylene PE 50 tubing (inner diameter, 0.58 mm; outer diameter, 0.965 mm) (Becton Dickinson, Sparks, MD). The capillaries were coated with P-selectin (20 μg/ml) or E-selectin (30 μg/ml) for 2 h and blocked for 1 h using 10% casein (Pierce Chemicals, Dallas, TX). The chamber was connected at one side to PE 10 tubing and inserted into the carotid artery, and a PE 50 tube on the other side was used to control the wall shear stress (5.94 dynes/cm^2). Microscopy was conducted using a Zeiss Axioskop microscope (Carl Zeiss, Inc., Thornwood, NY) with a saline immersion objective (SW 20/0.5). Images were recorded with a 3CCD color video camera (model DXC-390; Sony Corporation, Japan) connected to a Panasonic S-VHS recorder. The chamber was perfused with blood for 6 min before one representative field of view was recorded for 1 min.

B-cell activation and antibody production. B lymphocytes were purified from splenocytes by using a Dynal MPC magnet system (Dynal Biotech). Equivalent numbers of B cells of each genotype (1×10^5) were cultured in complete RPMI 1640 medium containing β-mercaptoethanol (0.1 mM), 10% FCS, and L-glutamine with the indicated concentrations of goat $F(ab')_2$ anti-mouse IgM antiserum (Jackson) or lipopolysaccharide (LPS; Sigma). Proliferative capacity was measured by cellular incorporation of [^{3}H]thymidine (2.5 μCi per well) during the last 16 h of a 72-h assay period.

Mice were bled to obtain preimmune sera and subsequently immunized by intraperitoneal injection of 100 μg of dinitrophenyl (DNP)-keyhole limpet hemocyanin (KLH) (Calbiochem) in Freund's complete adjuvant or 10 μg of DNP-Ficoll (Biosearch) in PBS. Serum was collected at the indicated times, and anti-DNP titers were determined by enzyme-linked immunosorbent assay, using plates coated with 20 μg of DNP-bovine serum albumin and blocked with 10% FCS in PBS. Mice receiving the DNP-KLH antigen were boosted at the indicated times with the same amount of antigen in Freund's incomplete adjuvant. Sera were diluted to various concentrations and analyzed using anti-mouse isotype-specific antibodies conjugated to alkaline phosphatase (IgM and IgA [Sigma] or IgG1, IgG2a, IgG2b, and IgG3 [Pharmingen]). Optical densities at 405 nm (OD_{405}) were obtained using a microplate reader (Molecular Devices). Results shown in Fig. 7 comprise the indicated serum dilutions in the linear range for the OD_{405} values obtained.

Peritonitis. Mice were administered 1 ml of 0.2% casein in PBS by intraperitoneal injection. At the indicated times, animals were sacrificed and their peritoneal cavities were subjected to lavage with 10 ml of ice-cold PBS containing 1% bovine serum albumin and 0.5 mM EDTA. Red blood cells were removed by ammonium chloride lysis. Peritoneal cell exudates were incubated with anti-Gr-1 antibody and the pan-macrophage marker antibody F4/80 and analyzed by flow cytometry.

Statistical analysis. Data were plotted as means ± standard errors of the means, and Student's *t* test was used to calculate *P* values, unless otherwise indicated.

RESULTS

Germ line mutagenesis of polypeptide GalNAcT-1 disrupts O-glycosylation activity. A genomic DNA clone encompassing exon 3 of the mouse gene encoding ppGalNAcT-1 was isolated, characterized by sequence analysis, and used in constructing a gene-targeting vector for conditional mutagenesis (Fig. 1A; see Fig. S1 in the supplemental material). Incorporation of loxP recombination signals flanking exon 3 and of selectable markers permitted modular excision by Cre recombinase activity, resulting in the presence of type 1 (Δ; deleted) and type 2 (*F*; loxP-flanked) alleles (Fig. 1B). Genomic DNA samples from embryonic stem (ES) cells bearing the targeted *F*[*tkneo*] allele were first characterized for the retention of all three loxP sites (Fig. 1C). Following Cre transfection, ES cell subclones bearing the expected type 1 and type 2 alleles were isolated. Mice bearing loxP-flanked exon 3 in the germ line (*ppGalNAcT-1^F*) were generated from ES cell clone 3-3 and were bred with Zp3-Cre transgenic mates (47) to produce offspring bearing the *ppGalNAcT-1$^\Delta$* allele (Fig. 1D). The *ppGalNAcT-1$^\Delta$* allele was then crossed into the C57BL/6NHsd inbred mouse background for at least six generations prior to phenotypic analysis. A minor but consistent reduction in the frequency of pups homozygous for the *ppGalNAcT-1$^\Delta$* allele was observed; however, those born developed to adulthood without overt physiologic abnormalities comparable to wild-type (*wt*/*wt*) and heterozygous (*wt*/Δ) littermates.

ppGalNAcT-1 enzymatic activity in extracts of multiple tissues of *wt*/*wt* and Δ/Δ mice at 8 weeks of age was measured using a peptide substrate that is O glycosylated preferentially by ppGalNAcT-1. Enzymatic activity was detected among multiple tissues from wild-type animals. In contrast, mice homozygous for the *ppGalNAcT-1$^\Delta$* allele lacked detectable ppGal NAcT-1 activity among all tissues surveyed, with the exception of the brain (Fig. 1E). The remaining enzyme activity in brain samples may reflect the expression of a closely related ppGal NAcT isozyme (22, 68). Deletion of exon 3 results in premature translational termination (Fig. 1F). Further confirmation that exon 3 deletion abolishes ppGalNAcT-1 enzyme activity was obtained upon expression of cDNA clones derived from mice bearing the *wt*/*wt* or Δ/Δ genotype. Significant enzymatic activity towards the peptide substrate in COS7 cell extracts was observed upon high-level expression of wild-type ppGal NAcT-1 cDNA, while significant activity was not detected upon similar RNA expression of a truncated ppGalNAcT-1 cDNA structure isolated from mice bearing the Δ/Δ genotype (Fig. 1G and data not shown). These findings reveal that deletion of ppGalNAcT-1 exon 3 results in an enzymatic null mutation.

Altered hemostasis and increased bleeding in ppGalNAcT-1-deficient mice. During routine tissue biopsies and surgical manipulations of ppGalNAcT-1-deficient mice, there was a significant increase in bleeding and hemorrhaging. We measured a threefold increase in bleeding time among mice lacking ppGalNAcT-1 (Table 1). Moreover, while the prothrombin time was normal, the activated partial thromboplastin time (APTT) was slightly prolonged by ppGalNAcT-1 deficiency. This suggested that ppGalNAcT-1 deficiency might alter coagulation factor levels or other hemostatic components of the blood, such as VWF and platelets. Coagulation factor activity levels in ppGalNAcT-1-deficient mice were indeed altered, with a slight to moderate decrease in most coagulation factors, including those that contribute to bleeding time and APTT measurements, such as factors V, VII, VIII, IX, X, and XII. In ppGalNAcT-1 deficiency, the VWF antigen level increased approximately 50%. The VWF produced by ppGalNAcT-1-deficient mice had a normal capacity to bind factor VIII but a slightly reduced (by 10%) capacity to bind collagen (data not shown). However, there was no apparent difference in PNA

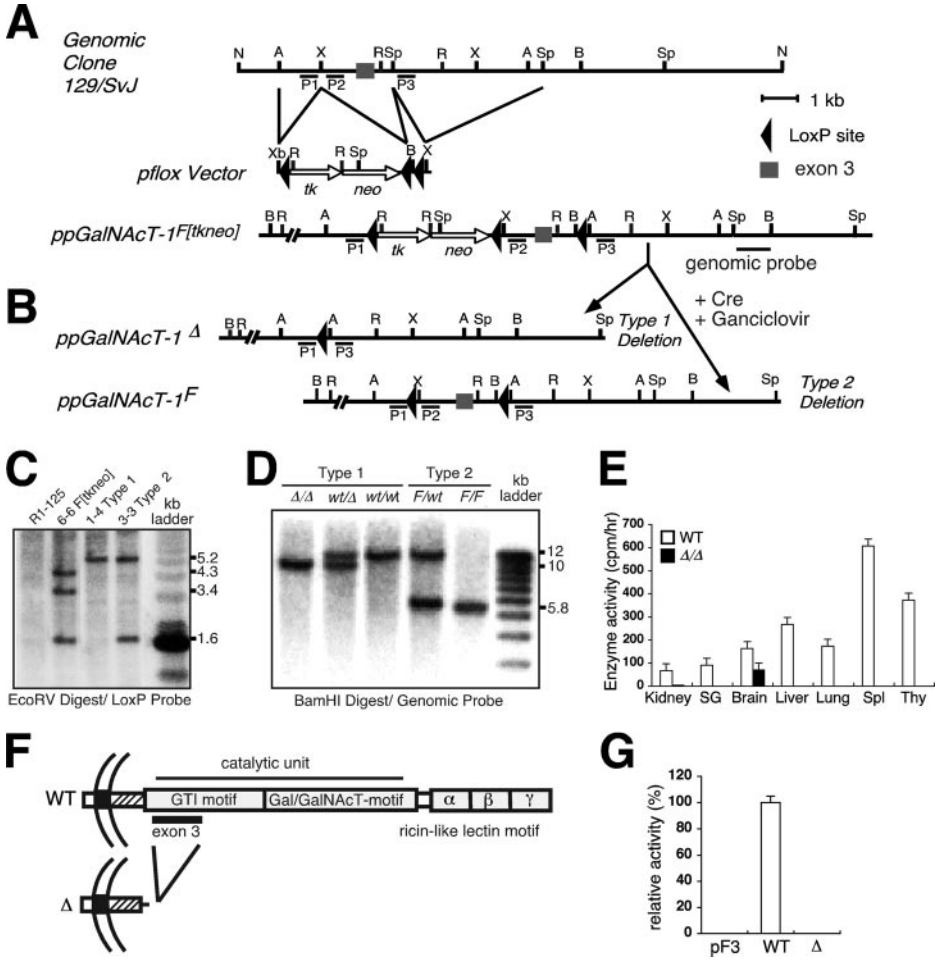

FIG. 1. ppGalNAcT-1 mutagenesis and loss of enzyme activity by deletion of exon 3. (A) Construction of ppGalNAcT-1 targeting vector for subsequent Cre-loxP recombination. (B) Cre recombination results in the deletion of exon 3, producing the null allele (type 1), or the flanking of exon 3 by loxP sites to generate the floxed allele (type 2). Restriction enzyme sites for panels A and B are indicated as follows: A, ApaI; B, BamHI; R, EcoRV; X, XhoI; Sp, SpeI; N, NotI. (C) Genomic Southern blot analysis of targeted ES cell clones (6-6, 1-4, and 3-3), using the loxP probe. (D) Genomic Southern blotting of tail DNAs, using a genomic probe, indicated the presence of germ line type 1 and type 2 mutations in the gene encoding ppGalNAcT-1. (E) Enzyme activity was assayed with total protein extracts from various tissues by using the peptide substrate PRFQDSSSKAPPPLPSPSRLPG. O-glycosylated products were profiled by anion-exchange chromatography and evaluated by reverse-phase high-performance liquid chromatography. Data are represented as means ± standard deviations (SD) for three separate experiments. SG, salivary gland; Spl, spleen; Thy, thymus. (F) Polypeptide GalNAcT-1 cDNA structures sequenced from the kidney tissues of mice bearing either the wild-type or deleted (Δ) allele. (G) ppGalNAcT enzyme activity towards the EA2 peptide (PTTDSTTPAPTTK) in COS7 cell extracts following transfection of cDNAs expressed by the pIMKF3 vector. Data are represented as means ± SD for three separate experiments. WT, wild type.

binding to VWF. Platelet counts (Fig. 2A) and platelet aggregation in response to various stimuli, including arachidonic acid, collagen, ADP, thromboxane analog, and calcium ionophore, were similar in both wild-type and null mice (data not shown). Whether these changes reflect a decreased rate of production or a decrease in half-life remains to be established.

ppGalNAcT-1 function in leukocyte homeostasis and O glycosylation. We carried out further initial phenotypic screening, including assessments of organ function by analysis of serum chemistry. While those measurements were within the normal range among ppGalNAcT-1-deficient mice (see Table S1 in the supplemental material; data not shown), alterations among white blood cell populations were detected (Fig. 2A). The number of lymphocytes in circulation was slightly increased, while eosinophils and basophils were substantially reduced. No change was seen in the circulating levels of $Gr1^+$ neutrophils. Similarly, platelet and red blood cell counts and the hemoglobin level were unaffected. The mean platelet volume, as well as red blood cell morphology and hemoglobin content, was also normal (data not shown).

O glycosylation initiated by ppGalNAcTs can be detected in part by the PNA lectin, which binds to the unsialylated core 1 O-glycan (44). Cytometric measurements of PNA binding at the cell surfaces of intact viable leukocytes revealed a significant decrease in O glycosylation among $Gr1^+$ neutrophils and $B220^+$ B cells, while no significant diminution occurred on the surfaces of $CD3^+$ T cells (Fig. 2B). These findings indicate that a loss of protein O glycosylation, as detected by PNA binding, occurs among some but not all leukocyte cell types.

TABLE 1. Hemostasis and coagulation

Parameter	Value[a]	
	Wild-type mice	ppGalNAcT-1-deficient mice
Time (s)		
Bleeding	75 ± 100	239 ± 257***
Prothrombin	10.3 ± 0.4	10.5 ± 0.3
APTT	26.8 ± 2.0	29.6 ± 3.6*
Protein level (% of wild-type BL/6 level)		
Antithrombin	136 ± 17	123 ± 16
Protein C	85 ± 15	84 ± 22
Protein S	153 ± 102	166 ± 112
Plasminogen	77 ± 11	66 ± 14*
Alpha-2 antiplasmin	121 ± 26	107 ± 17
Factor II	109 ± 36	103 ± 19
Factor V	124 ± 17	105 ± 17*
Factor VII	88 ± 17	71 ± 16*
Factor VIII	104 ± 28	70 ± 15*
Factor IX	88 ± 15	65 ± 6**
Factor X	102 ± 21	86 ± 17*
Factor XI	84 ± 14	69 ± 21
Factor XII	105 ± 16	85 ± 14*
VWF	204 ± 64	296 ± 136***

[a] Results are expressed as means ± SD (***, $P < 0.001$; **, $P < 0.01$; *, $P < 0.05$). The number of samples studied was 14 for wild-type mice and 10 for ppGalNAcT-1-deficient mice, except for bleeding time analysis. For that analysis, the number of mice studied was 39 for wild-type mice and 34 for ppGalNAcT-1-deficient mice.

ppGalNAcT-1 contributes to E- and P-selectin ligand formation and neutrophil recruitment during inflammation. Circulating Gr-1$^+$ neutrophils were further analyzed for the levels of E- and P-selectin ligands at the cell surface by flow cytometry. Remarkably, the relative reduction in neutrophil cell surface O-glycans judged by PNA lectin binding was accompanied by a fourfold decrease in E-selectin ligand expression and a fivefold reduction in P-selectin ligand levels (Fig. 3A). No changes occurred in the expression of other cell surface molecules involved in cell adhesion, including CD11, CD18, and L-selectin as well as the selectin counterreceptors CD24 and PSGL-1 (Fig. 3B).

To investigate the effect of reduced selectin ligand expression on the adhesive properties of neutrophils, E- and P-selectin-mediated leukocyte rolling was measured using an autoperfused flow chamber (67). The number of ppGalNAcT-1-deficient leukocytes rolling on P-selectin was reduced to approximately 50% of the normal level, whereas the number of cells rolling on E-selectin was reduced to approximately 30% of the normal level, at 5.94 dynes/cm^2 (Fig. 3C).

The impact of this deficiency in E- and P-selectin ligands upon neutrophil recruitment to an inflammatory stimulus was explored in a model of acute peritonitis. A significant decrease in intraperitoneal neutrophil recruitment reflecting a three- to fivefold reduction in Gr-1$^+$ cell number resulted from the absence of ppGalNAcT-1 (Fig. 3D). This finding is consistent with the observed reductions of E- and especially P-selectin ligand levels with diminished leukocyte rolling, indicating that protein O glycosylation contributed by ppGalNAcT-1 plays a significant role in the formation of selectin ligands that operate in the innate immune inflammatory response among activated endothelial cells.

Selectin ligand formation by ppGalNAcT-1 promotes lymphocyte homeostasis, L-selectin ligand formation, and trafficking to lymph nodes. Elevated levels of lymphocytes in the blood of ppGalNAcT-1-deficient mice reflected an increase in both T- and B-lymphocyte numbers (Fig. 4A). Moreover, reduced total cellularity was detected among the lymph nodes, while no changes in cellularity occurred within the spleen, thymus, bone marrow, and Peyer's patch tissues (Fig. 4B). Mesenteric, cervical, and axillary lymph nodes were reduced in total cellularity by an average of 60%, while the inguinal lymph node lost 90% of the normal cell number and, in some cases, was anatomically absent. Characterization of cell populations within the lymph nodes revealed deficiencies in both T and B lymphocytes, although B-lymphocyte numbers were most severely reduced, by 50 to 95% (Fig. 4C). T-lymphocyte cellularity was also reduced, but not as markedly, with the exception of the inguinal lymph node tissue (Fig. 4D).

Lymph node architecture, comprising cellular and molecular determinants, was examined among lymphocyte subpopulations and endothelial cells that express selectin ligands. A reduced anatomic size and reduced numbers of lymph node follicles were observed for ppGalNAcT-1 deficiency, with no apparent change in the follicular trafficking pattern of B and T cells (Fig. 5A). Levels of L-selectin receptors on the surfaces of

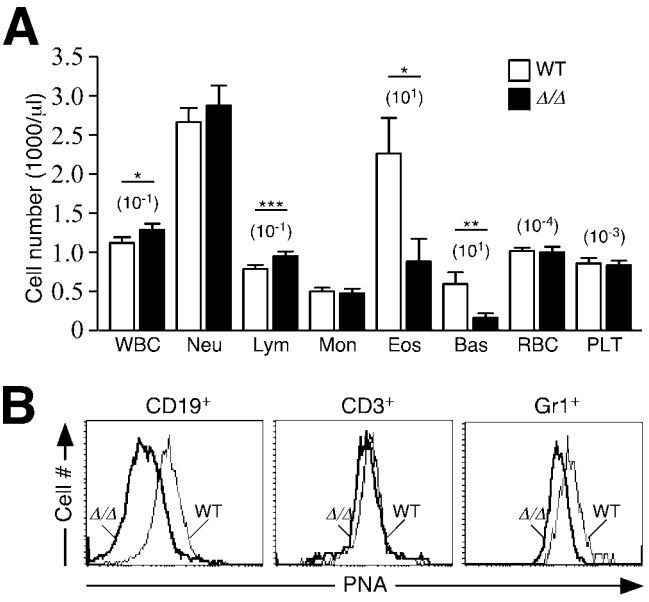

FIG. 2. Altered blood lymphocyte levels with reduced protein O glycosylation. (A) Leukocyte counts were obtained from blood of wild-type and ppGalNAcT-1-deficient mice. Cell numbers are expressed as means per μl of whole blood ± standard errors of the means (SEM) among 21 mice, including littermates of the indicated genotypes. WBC, white blood cell; Neu, neutrophil; Lym, lymphocyte; Mon, monocyte; Eos, eosinophil; Bas, basophil; RBC, red blood cell; Plt, platelet. An unpaired *t* test indicated significance (***, $P < 0.001$; *, $P < 0.05$). (B) Reduced protein O glycosylation on the cell surfaces of circulating leukocytes, detected by PNA lectin binding. Reduced PNA binding was observed among Gr1$^+$ neutrophils and B220$^+$ B cells. In contrast, close-to-wild-type levels of O-glycans detected by PNA binding levels were noted among unactivated circulating CD3$^+$ T cells. WT, wild type.

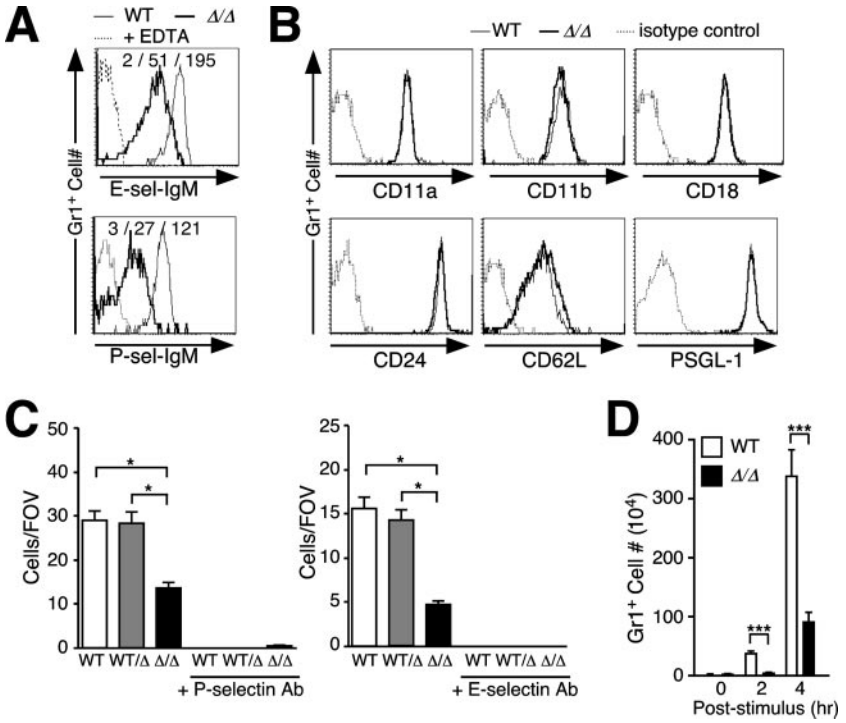

FIG. 3. Reduced selectin ligand expression on ppGalNAcT-1-deficient neutrophils attenuates selectin-mediated rolling and inflammation in a model of acute peritonitis. (A) Reduced E- and P-selectin ligands among circulating $Gr1^+$ cells, detected by selectin-IgM chimera binding and flow cytometry. Loss of selectin-IgM chimera binding in the presence of EDTA is also shown. (B) Expression levels of adhesion molecules (CD11a, CD11b, CD18, and CD62L) and selectin counterreceptors (CD24 and PSGL-1) on $Gr1^+$ cells in blood, analyzed by flow cytometry. The results shown in panels A and B are representative of three experiments with separate littermates. (C) Numbers of rolling leukocytes on P-selectin and E-selectin were reduced in ppGalNAcT-1-deficient mice, analyzed using blood-perfused microflow chambers at 5.9 dynes/cm^2. Data presented are means ± SEM for at least six chambers, using cells from three separate littermates of the indicated genotypes. *, $P < 0.05$ compared to ppGal NAcT-1. FOV, field of view. (D) Peritoneal cells were collected, and $Gr1^+$ neutrophils were counted prior to (0 h) or after (2 or 4 h) intraperitoneal injection of casein to initiate acute peritonitis. Data are presented as means ± SEM for eight mice representing littermates of the indicated genotypes (***, $P < 0.001$). WT, wild type.

T and B cells from various compartments were analyzed and found to be normal (Fig. 5B). In contrast, L-selectin ligands that are normally expressed on high endothelial venules (HEVs) were significantly reduced in the absence of ppGal NAcT-1 among mesenteric and inguinal lymph nodes (Fig. 5C). The inguinal node was the most severely affected node compared with mesenteric lymph node tissue. Approximately 10% of normal L-selectin ligand expression remained among inguinal lymph nodes, while close to 60% of normal L-selectin ligand levels remained among mesenteric lymph nodes (Fig. 5D). Interestingly, a significant decrease in MECA-79 antibody binding occurred only among inguinal HEVs, while normal MECA-79 levels were expressed among mesenteric lymph nodes. The degrees of L-selectin ligand deficiency among different lymphoid aggregates were proportional to the degrees of reduced lymphocyte cellularity observed, implicating reduced L-selectin ligand levels in lymph node HEVs as being responsible for reduced cellularity. Attempts to further investigate leukocyte adhesion by intravital microscopy were unsuccessful due to the extensive bleeding and hemorrhaging that occurred during surgery, as noted above. Nevertheless, the efficacy of lymphocyte homing could be measured.

Isolated T and B cells from wild-type mice were covalently labeled using CMFDA and injected into the tail veins of syngeneic wild-type and ppGalNAcT-1-deficient littermate recipients. Levels of CMFDA-labeled lymphocytes among lymphoid aggregates were analyzed 1 h and 24 h following transfer. CMFDA-labeled B and T lymphocytes were detected in all lymphoid tissues surveyed within 1 h. However, a significant reduction in B-cell homing was observed among ppGalNAcT-1-deficient recipients, with the exception of Peyer's patch tissue (Fig. 6A). At 24 h posttransplantation, the most severe B-cell homing deficit continued to involve the inguinal lymph nodes of recipients, followed in severity by homing to axillary, cervical, and mesenteric lymph nodes, with a normal homing frequency for Peyer's patch tissue (Fig. 6B). Lesser but significant deficits in T-cell homing were also observed and occurred with a similar profile, with the most significant decrease in homing to the inguinal lymph nodes. These findings reveal that the reduced cellularity among lymph nodes is proportional to the severity of the lymphocyte homing defect and tracks with the degree of L-selectin ligand deficiency among the HEVs of ppGalNAcT-1-deficient recipients.

ppGalNAcT-1 supports IgG production in the humoral immune response. Circulating levels of Ig isotypes IgG1, IgG2a, and IgG3 were significantly reduced in the sera of ppGal NAcT-1-deficient mice, while normal levels of IgM and IgA

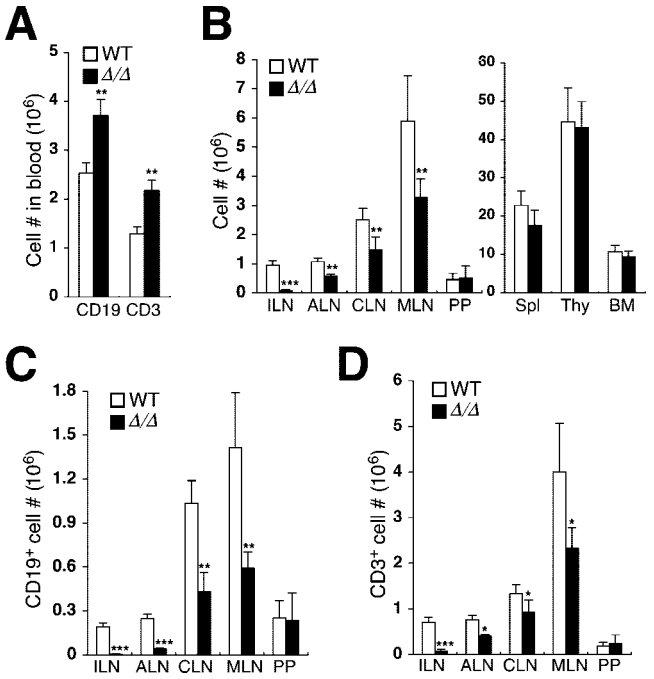

FIG. 4. Leukocytosis involving T and B cells is associated with a reduction in lymph node cellularity. (A) Circulating numbers of T cells ($CD3^+$) and B cells ($CD19^+$) were significantly increased in ppGalNAcT-1-deficient mice. (B) Leukocyte abundance was reduced among distinct peripheral lymphoid aggregates, including inguinal lymph nodes (ILN), axillary lymph nodes (ALN), cervical lymph nodes (CLN), and mesenteric lymph nodes (MLN). No significant change occurred among the Peyer's patch (PP), spleen (Spl), thymus (Thy), and bone marrow (BM) compartments. (C) B-lymphocyte ($CD19^+$) numbers were significantly reduced among multiple lymphoid aggregates. (D) T-lymphocyte ($CD3^+$) numbers were reduced most significantly among inguinal lymph nodes. Data are means ± SEM for 12 littermate pairs of the indicated genotypes. An unpaired *t* test indicated significance (***, $P < 0.001$; **, $P < 0.01$; *, $P < 0.05$). WT, wild type.

were detected (Fig. 7A). It seemed unlikely that this effect was due to a reduction in L-selectin function, as such animals have been reported to express normal to elevated Ig levels and to exhibit a robust humoral immune response (2, 49). We further noted that B-cell surface expression of major histocompatibility complex class II and costimulatory molecules CD40, CD44, and B7.2 was unaltered in the absence of ppGalNAcT-1 (Fig. 7B). Moreover, B-cell proliferation responses to LPS or antibody-mediated IgM cross-linking were also unaffected (Fig. 7C). In contrast, upon immunization with the T-cell-independent antigen DNP-Ficoll, ppGalNAcT-1-deficient mice failed to induce a significant IgG antibody titer in the presence of normal titer increases involving IgM and IgA isotypes (Fig. 7D). Similarly, a deficit of anti-DNP IgG antibody production was detected following immunization with the T-cell-dependent antigen DNP-KLH (Fig. 7E).

ppGalNAcT-1 deficiency attenuates GC formation upon immunization. The development of B cells that can express IgG isotypes takes place within GCs of follicles within peripheral lymphoid tissues in response to antigenic exposure. The GC microenvironment is essential for Ig isotype class switching and affinity maturation in producing plasma B cells that provide the circulating repertoire of IgG antibodies. Following immunization of ppGalNAcT-1-deficient mice, we noted a threefold reduction in the numbers of detectable GCs within the white pulp of the spleen and lymph nodes compared with the numbers for wild-type littermates (Fig. 8A). Localization of B and T cells and expression of $FDCM1^+$ dendritic cells appeared unaltered among follicles of ppGalNAcT-1-deficient mice (Fig. 8B). Although GC B cells were detected with the antibody GL7 and decreased IgD expression resulted as expected (not shown), another marker of GC B cells, the PNA lectin (31), could not detect GC B cells in ppGalNAcT-1-deficient tissues (Fig. 8C). This finding indicates that ppGalNAcT-1 is essential for synthesizing O-glycans among GC B cells that are typically detected by PNA binding. In addition, splenic B-cell levels as well as $GL7^+$ GC B-cell numbers were significantly decreased in ppGalNAcT-1 deficiency at 8 days postimmunization (Fig. 8D). These results indicate that ppGalNAcT-1 deficiency significantly decreases O-glycans on GC B cells that normally bear PNA lectin binding determinants and further diminishes the number of GC B cells, with reduced GC formation.

Increased apoptosis of GC B cells in ppGalNAcT-1 deficiency. The reductions in frequency of GCs and total GC B cells in ppGalNAcT-1-deficient mice did not appear to be due to impaired B-cell proliferation. Either by ex vivo B-cell stimulation assays or by in situ analysis of GC expression of the nuclear proliferation marker Ki-67, B cells lacking ppGal NAcT-1 appeared unaltered in their responses to stimuli that lead to cell proliferation (Fig. 7C and data not shown). However, a reduction in GC B cells was associated with an increased frequency of $CD68^+$ tingible-body macrophages. Cellular markers of apoptosis were significantly induced in GCs from ppGalNAcT-1-deficient mice. Activated caspase-3 and DNA fragmentation detected by TUNEL were greatly elevated and often colocalized with $CD68^+$ macrophages (Fig. 9A to C). The GC has a polar two-compartment structure, including a dark zone (centroblasts) and a light zone (centrocytes). The dark zone is proximal to the T-cell area and contains rapidly dividing Ig^- B cells called centroblasts, while the light zone contains Ig^+ centrocytes, which undergo selection based on the affinity of their Ig receptor for the antigen. Following immunization, centroblasts and centrocytes were measured as previously described (64). An alteration in the frequency of viable centroblasts and centrocytes was observed, reflecting a significant reduction in centrocyte number (Fig. 9D). This was accompanied by significant increases in activated caspase-3 abundance among centrocytes, and especially centroblasts, during ppGalNAcT-1 deficiency (Fig. 9E).

IgG abundance was significantly reduced among GCs in ppGalNAcT-1-deficient tissues, in the context of increased apoptosis among IgG-positive cells (Fig. 10A). Moreover, reduced numbers of IgG^+ B lymphocytes were observed in the spleens of immunized ppGalNAcT-1-deficient mice (Fig. 10B). In addition, the frequency and number of plasma B cells were also markedly reduced (Fig. 10C). These findings establish an essential role of ppGalNAcT-1 in promoting plasma B-cell abundance and IgG formation by moderating the apoptosis of centrocytes bearing IgGs among GC B cells.

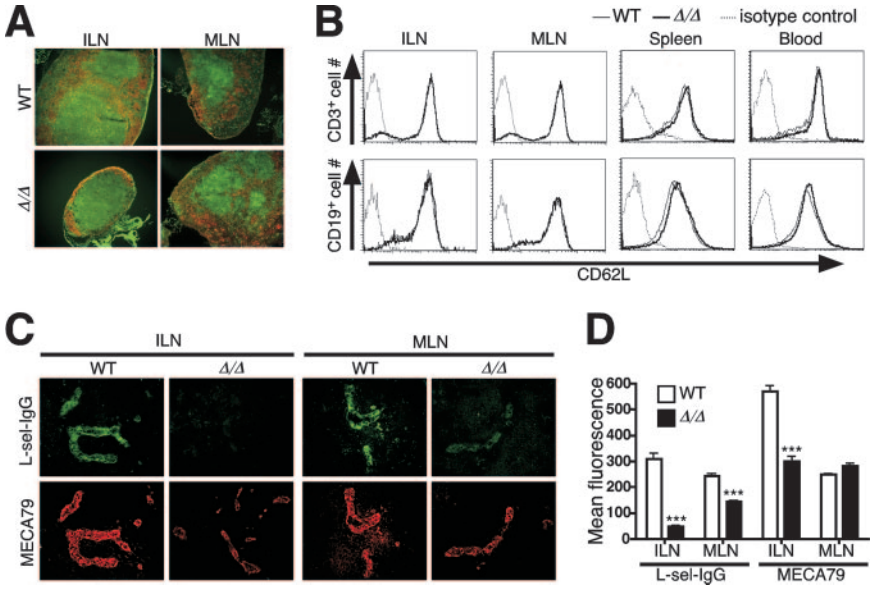

FIG. 5. Tissue-selective deficiency in L-selectin ligand and MECA-79 epitope expression among peripheral lymph nodes. (A) Histological analysis of inguinal (ILN) and mesenteric (MLN) lymph nodes incubated with CD4-FITC, CD8-FITC, and B220-Rho and visualized by fluorescence microscopy. Magnification, ×100. (B) Unaltered expression levels of L-selectin on $CD19^+$ and $CD3^+$ lymphocytes in spleen, blood, and inguinal and mesenteric lymph nodes, as indicated by flow cytometry. Dotted lines represent background cell fluorescence using isotype-specific control antibodies. (C) Frozen sections of inguinal and mesenteric lymph nodes stained with L-selectin–IgG chimera or MECA-79 antibody. Magnification, ×400. (D) Relative levels of L-selectin ligands and MECA-79 expression on HEVs were obtained by quantifying fluorescent signals from serial and parallel tissue sections of inguinal lymph nodes (ILN) and mesenteric lymph nodes (MLN), using deconvolution microscopy and MetaMorph software analysis (see Materials and Methods). WT, wild type.

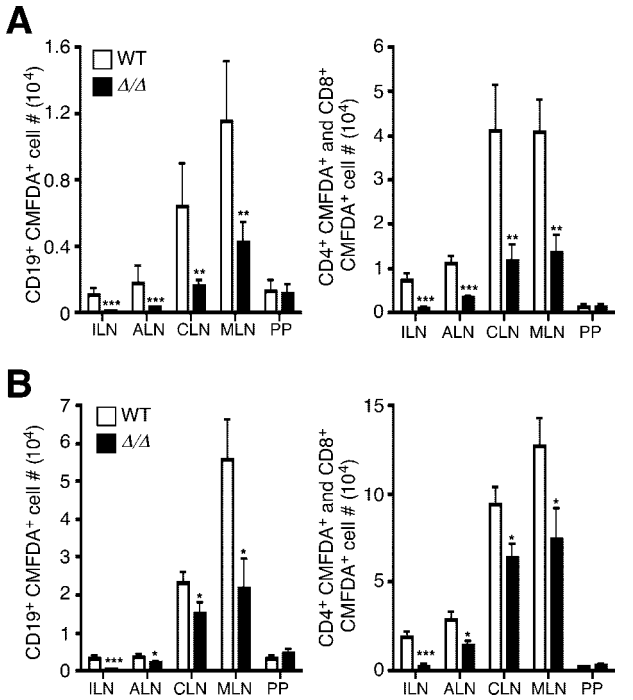

FIG. 6. ppGalNAcT-1 supports lymphocyte homing to specific lymph nodes. CMFDA-labeled lymphocytes (2.5×10^7) obtained from wild-type (WT) mice were injected into the tail veins of recipients of the indicated genotypes. Lymphoid aggregates, as denoted in the legend to Fig. 4, were harvested 1 h (A) or 24 h (B) after injection. $CMFDA^+$ T and B lymphocytes were quantified by flow cytometry. Data are means ± SEM for eight mice of each genotype. An unpaired *t* test indicated significance (***, $P < 0.001$; **, $P < 0.01$; *, $P < 0.05$).

DISCUSSION

A significant proportion of nascent vertebrate proteins transiting the secretory pathway are O glycosylated by the action of one or more members of a conserved family of ppGalNAcTs. Different genes encode the various ppGalNAcTs among all multicellular organisms surveyed, and thus it appears likely that important and often nonoverlapping physiologic activities will be attributed to individual members of this glycosyltransferase family (34). The production and study of intact organisms that lack individual ppGalNAcTs, including nematodes, insects, rodents, and primates, reveal remarkable cell type specificity in the phenotypes and pathologies arising from these deficiencies. Although ppGalNAcT-1 was the first member of the ppGalNAcT family to be identified and characterized because it is highly expressed among many cell types, the biological roles of this glycosyltransferase in mammalian development and physiology have remained unknown. By engineering an inheritable germ line mutation in the mouse gene that disables ppGalNAcT-1 function, we have established a ppGal NAcT-1 deficiency state for initial and future investigations into the biology of core-type protein O glycosylation contributed by this highly conserved glycosyltransferase. Our analyses thus far have shown that ppGalNAcT-1 markedly supports the activities of glycoproteins that contribute to blood coagulation, selectin-mediated leukocyte trafficking and inflammation, and GC B-cell apoptosis in modulation of the humoral immune response. Although decreased B-cell trafficking to lymph nodes and increased apoptosis do not appear to be connected mechanistically, they are likely collaborative in the observed reduction of humoral immunity. The focus of ppGalNAcT-1 func-

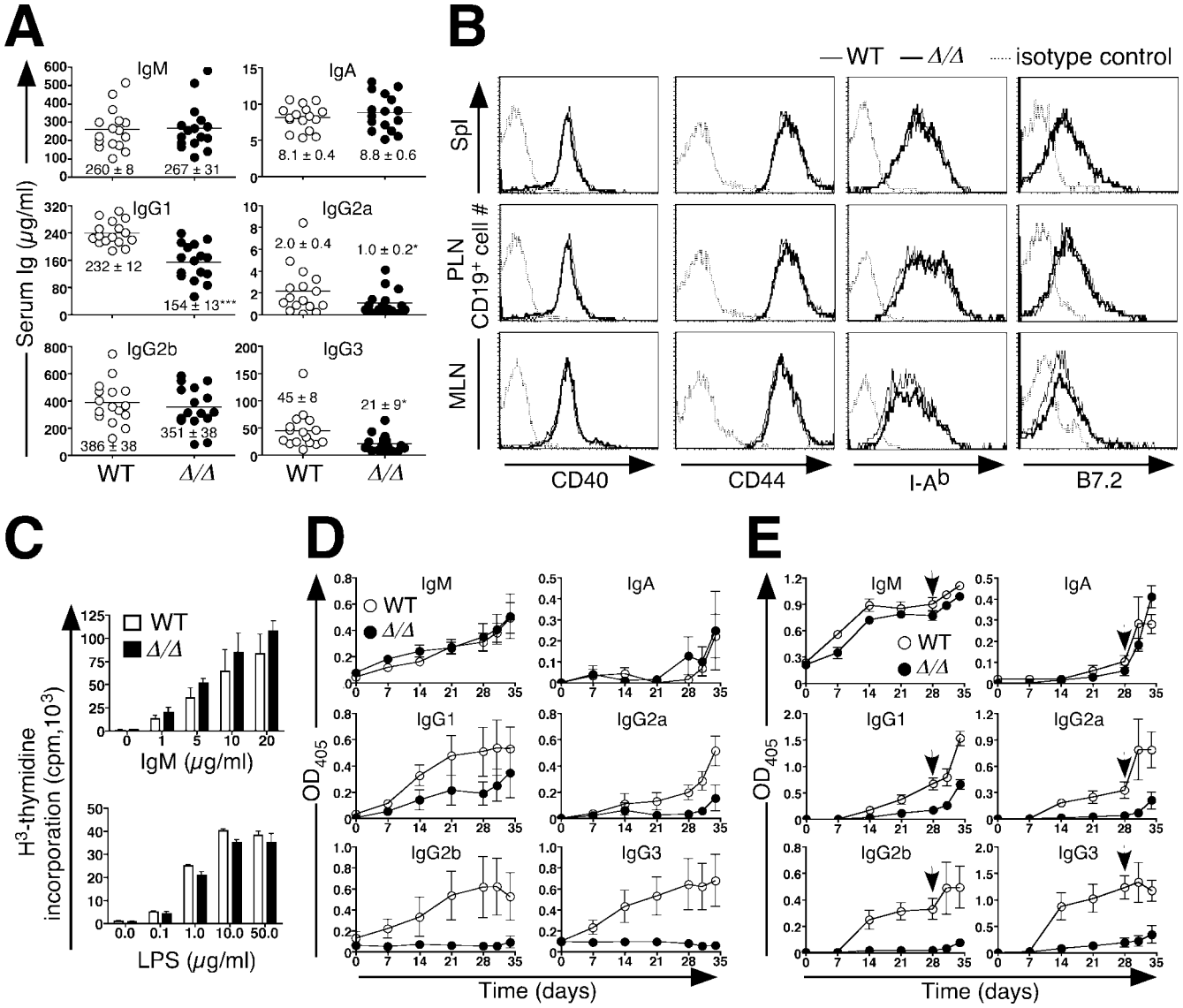

FIG. 7. Normal antigen receptor activation contrasts with attenuated antibody production due to loss of ppGalNAcT-1. (A) Serum Ig levels among 8-week-old naive mice ($n = 16$). Points represent measurements for individual animals. The median Ig levels are depicted as horizontal bars (means ± SEM are indicated). An unpaired t test indicated significance (***, $P < 0.001$; *, $P < 0.05$). (B) The expression levels of activation markers (CD44, B7.2, and I-A^b) and CD40 were analyzed by flow cytometry on CD19$^+$ lymphocytes derived from the spleen (Spl), peripheral lymph nodes (PLN), and mesenteric lymph nodes (MLN). The results shown are representative of three separate experiments. Dotted lines represent the fluorescence of cells stained using an isotype-specific control antibody. (C) B lymphocytes were isolated and stimulated by antibody to IgM or LPS. The proliferation response was measured by [^{3}H]thymidine incorporation. Data are presented as means ± SEM for three mice of the indicated genotypes. (D) Anti-DNP antibody levels produced in response to immunization with 10 μg of the T-cell-independent antigen DNP-Ficoll, measured at the indicated times. (E) Anti-DNP antibody levels measured before and subsequent to a secondary immunization (arrow) using 100 μg of the T-cell-dependent antigen DNP-KLH. Multiple dilutions of sera were assayed, with the results shown reflecting the linear range of responses (OD_{405} measurements) (data not shown). Data are presented as means ± SEM for eight mice of the indicated genotypes. WT, wild type.

tion upon selected cell types and glycoproteins enables further studies on the precise mechanisms by which the initiation of protein O glycosylation by ppGalNAcT-1 plays an advantageous role in vascular and immune responses. Although advantageous roles of ppGalNAcT-1 in physiology are evident, they appear to be dispensable for normal development and reproduction among laboratory-raised animals (32, 37). Moreover, inhibition of ppGalNAcT-1 activity may have therapeutic potential for some pathogenic syndromes involving increased thrombosis, chronic inflammation, and immunologic diseases of B lymphocytes.

In modulating blood coagulation levels, mild to moderate decreases in circulating levels of factors V, VII, VIII, IX, X, and XII, resulting in a prolonged APTT and bleeding time, were evident in ppGalNAcT-1 deficiency. The reduced level of factor VIII in the presence of an elevated level of VWF was a surprising result, since elevated levels of VWF tend to raise factor VIII levels. We found that VWF produced by ppGal

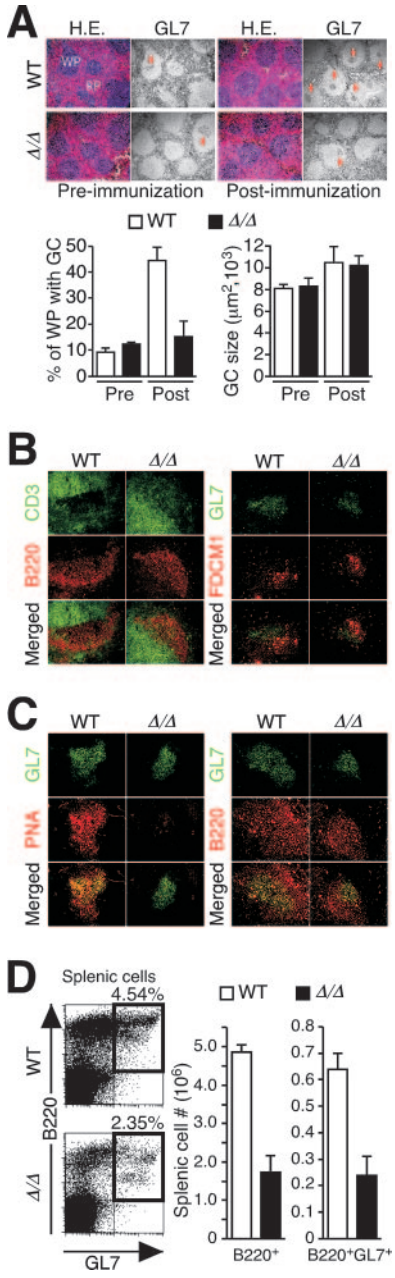

FIG. 8. Diminished GC development and B-cell expansion upon immunization of ppGalNAcT-1-deficient mice. (A) Splenic follicles and GCs from mouse spleens prior to and 8 days subsequent to immunization with DNP-KLH were detected with hematoxylin and eosin (H.E.) and with GL7 antibody. WP and RP indicate white pulp and red pulp, respectively. Images were magnified 100×. Small arrows within white pulp denote GC B cells. The percentage of white pulp bearing GCs and the size of GCs were measured. (B) GC B cells in the spleen were further analyzed in situ 14 days after immunization with DNP-KLH. T- and B-cell zones remained intact, and follicular dendritic cells (FDCM1$^+$) were present at normal levels. (C) GC markers include GL7 antibody binding among B220$^+$ B cells, while PNA binding dependent upon O glycosylation was substantially decreased in ppGalNAcT-1-deficient mice. Magnification (B and C), ×400. (D) Reduced frequency of splenic GC B cells (B220$^+$ GL7$^+$) as well as reduced total splenic B220$^+$ B-cell number among ppGalNAcT-1-deficient mice 8 days after immunization with DNP-KLH. Results shown are representative of data obtained from analyses of three to six littermates of the indicated genotypes. WT, wild type.

NAcT-1-deficient mice has a normal capacity to bind factor VIII but has a slightly reduced (by 10%) capacity to bind collagen (data not shown). Typically, elevated VWF levels are not associated with increased bleeding times. Thus, it is likely that the reductions in multiple coagulation factors, namely, factors V, VII, VIII, IX, and X, contribute to the hemostatic defects seen in the null mice. Since O glycosylation is not linked at present to cellular mechanisms that control protein synthesis and maturation in the secretory pathway, it is possible that ppGalNAcT-1 modulates binding activities, postsecretion proteolysis, and turnover among various O glycoproteins in circulation. Platelet homeostasis, in contrast, appeared to be unaffected by ppGalNAcT-1 deficiency. Besides the presence of normal platelet counts in circulation, no difference in aggregation or activation occurred in response to various stimuli, including arachidonic acid, collagen, ADP, thromboxane analog, and calcium ionophore (data not shown). Nevertheless, the prolonged bleeding time may reflect both altered coagulation factor levels and a reduced level of P-selectin ligand formation, which may diminish platelet function in hemostasis.

ppGalNAcT-1 further contributes to selectin ligand synthesis, supporting the formation of a significant proportion of ligands for E- and P-selectins on Gr-1$^+$ neutrophils in circulation as well as L-selectin ligands produced among lymph node HEVs. In comparison to the case for mice lacking core 2 GlcNAcT-1 (11), there remained slightly higher levels of both E- and P-selectin ligands on neutrophils lacking ppGalNAcT-1. This may explain the absence of neutrophilia in ppGalNAcT-1-deficient mice, which exists among animals lacking core 2 GlcNAcT-1. This implies that core 2 GlcNAcT-1-dependent E- and P-selectin ligand synthesis can occur at sites of protein O glycosylation initiated by other ppGalNAcT isozymes expressed in neutrophils. Nevertheless, the loss of ppGalNAcT-1 has a surprisingly severe impact on neutrophil recruitment in an acute peritonitis model of endothelial inflammation, with a degree of reduction in neutrophil influx comparable to that seen in animals lacking a larger apparent proportion of selectin ligands in the absence of either core 2 GlcNAcT-1 or fucosyltransferase (FT) VII.

The absence of ppGalNAcT-1 impairs T- and especially B-lymphocyte homing among peripheral lymphoid aggregates, including axial, cervical, mesenteric, and inguinal lymph nodes, resulting in a reduced number of lymphocytes among peripheral lymph node tissues. These findings were proportional to the degree of L-selectin ligand deficiency in vivo among the HEVs of various peripheral lymphoid aggregates. L-selectin ligand synthesis is controlled by the actions of glycosyltransferases and sulfotransferases, which construct 6-sulfo-sialyl Lewis^X (sLe^X) on glycan branches of several HEV-resident sLe^X counterreceptors, including GlyCAM-1, CD34, podocalyxin, Sgp200, endoglycan, and MAdCAM-1 (14, 43). Collaborative and differential roles for each class of enzyme have been observed in selectin ligand formation, involving lymphocyte homing and retention among peripheral lymph nodes (15, 21, 23). Glycoproteins bearing L-selectin ligands are typically O glycosylated and have mucin-like domains for multiple *O*-GalNAc linkages that act as the initial scaffolds. L-selectin ligands can be constructed on core 1- and core 2-type O-glycan branches, the former of which also harbor the MECA-79 antigen and are prominent in the absence of core 2 GlcNAcT-1

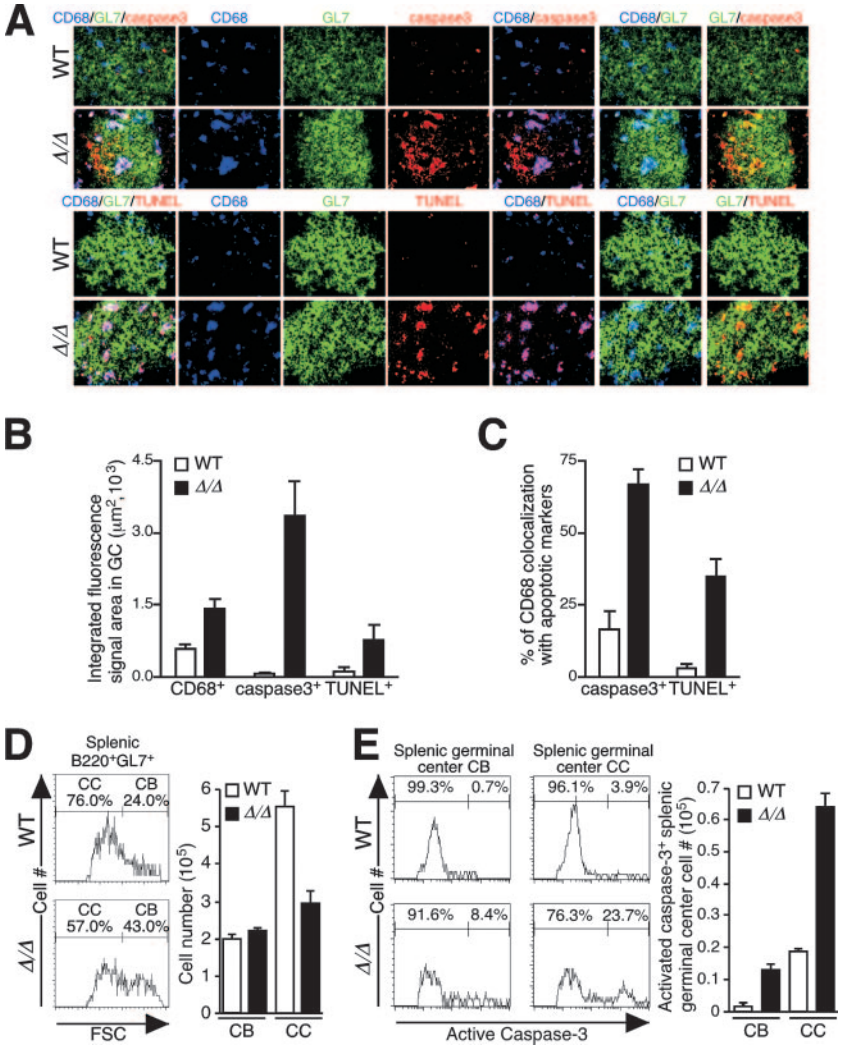

FIG. 9. Loss of O-glycans produced by ppGalNAcT-1-deficient mice increases GC macrophage infiltration and B-cell apoptosis. (A) Abundances of tingible-body macrophages ($CD68^+$) and markers of cell apoptosis, including activated caspase-3 and TUNEL, were increased in ppGalNAcT-1 deficiency among GC B cells analyzed in situ 14 days after immunization with DNP-KLH. Magnification, ×1,000. (B) CD68, activated caspase-3, and TUNEL measurements obtained by quantifying fluorescent signals. (C) Percentage of $CD68^+$ macrophage colocalization with apoptotic cell markers, including activated caspase-3 and TUNEL. (D) Centroblast (CB) and centrocyte (CC) populations among splenic GC B cells ($B220^+$ $GL7^+$) measured 8 days after immunization with DNP-KLH by forward-scatter (FSC) flow cytometry. (E) Increased abundance of activated caspase-3 detected among permeabilized centroblasts and centrocytes from ppGalNAcT-1-deficient mice by flow cytometry. Analyses were accomplished 8 days after immunization with DNP-KLH. Experiments shown are representative of data obtained from three to six littermates of the indicated genotypes. WT, wild type.

(65). Interestingly, normal levels of MECA-79 expression were detected among mesenteric lymph nodes of ppGalNAcT-1-deficient mice in the presence of a moderate reduction in L-selectin ligands, implying that mesenteric L-selectin ligands generated by ppGalNAcT-1 may lack the MECA-79 determinant. While glycosyltransferases other than ppGalNAcT-1 contribute to L-selectin ligand formation, L-selectin ligands produced within the inguinal lymph node are particularly dependent upon ppGalNAcT-1. The diminished level of L-selectin ligands is likely involved in the reduction of lymphocyte homing and abundance among various lymphoid aggregates during ppGalNAcT-1 deficiency.

Selective differences in the homing abilities of T and B cells have been described, independent of their site of origin, among the spleen, peripheral lymph nodes, mesenteric lymph nodes, and Peyer's patches (50). L-selectin expression levels appear to be a key contributor to this effect, as T lymphocytes express a twofold higher level of L-selectin than do B lymphocytes and are more efficient at homing to peripheral lymph nodes (50, 52). The absence of L-selectin expression on lymphocytes markedly reduces both T- and B-lymphocyte homing and localization among peripheral lymph nodes, as expected, but does not significantly alter lymphocyte numbers in circulation or among mesenteric lymph nodes, the spleen, or thymus tissue (2). Other distinctions are apparent. Splenomegaly is observed in L-selectin deficiency, but not among ppGalNAcT-1-deficient mice. The lesser defect in cellularity observed among mesenteric lymph nodes in ppGalNAcT-1 deficiency may re-

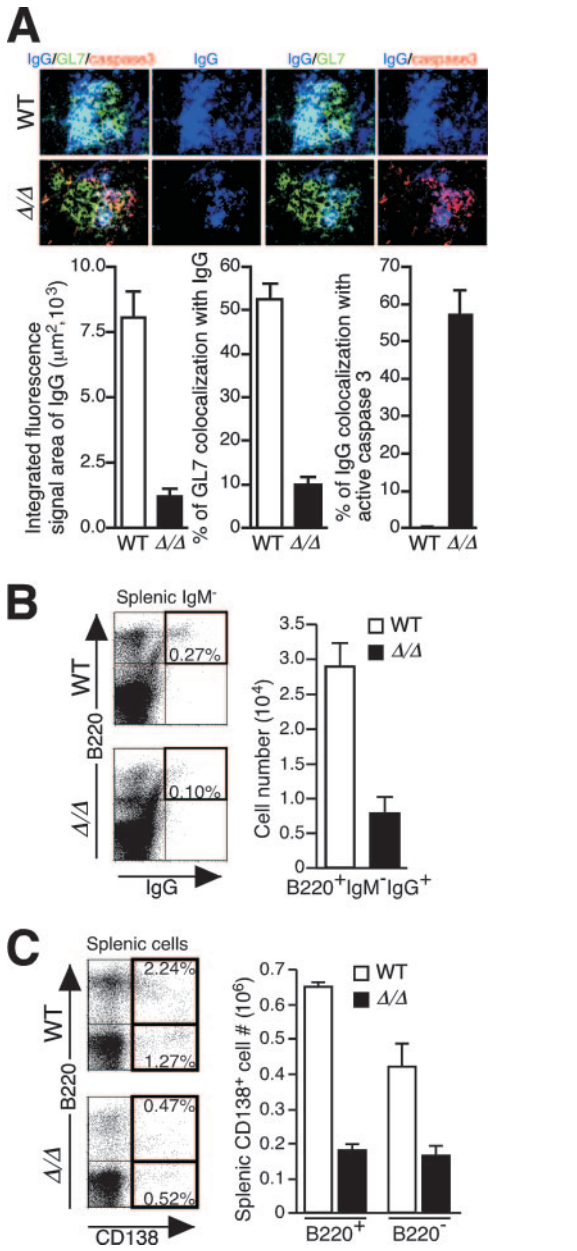

FIG. 10. Reduced IgG and plasma B-cell abundances during ppGalNAcT-1 deficiency. (A) Splenic GCs analyzed 14 days after immunization with DNP-KLH, indicating a reduced abundance of IgG as well as colocalization of the apoptosis marker activated caspase-3 with IgG-expressing B cells. Magnification, ×1,000. (B) Reduced frequency and number of viable IgG^+ IgM^- $B220^+$ B cells in the spleens of ppGalNAcT-1-deficient mice 8 days after immunization with DNP-KLH. (C) Reduced frequency and number of splenic plasma B cells ($CD138^+$) in ppGalNAcT-1-deficient mice, measured 8 days after immunization with DNP-KLH. Experiments shown are representative of data obtained from analyses of three to six littermates of the indicated genotypes.

flect the additional role of MAdCAM-1 as a ligand for the α4β7 integrin expressed on lymphocytes (6).

Multiple glycosyltransferases have been identified directly as participants in L-selectin ligand synthesis in vivo and previously included ST3Gal-IV, core 2 GlcNAcT-1, core 1 GlcNAcT, FT IV, and FT VII. Their individual and combined contributions modulate selectin ligand synthesis differentially among various cell types in vivo, often markedly reducing lymphocyte homing activity to lymph nodes (11, 13, 15, 25, 33, 36). The absence of both FT IV and FT VII results in a profound loss of lymphocyte numbers within peripheral lymph nodes, and animals lacking these factors have impaired T-cell-mediated immune responses (25, 39). Among core 2 GlcNAcT-1-deficient mice, a lesser reduction in B-cell (28%) than in T-cell numbers was reported for peripheral lymph nodes (15). The loss of ppGalNAcT-1 by itself has a remarkably severe impact on both leukocyte homing to HEVs and homeostatic peripheral lymph node cellularity, unlike other single glycosyltransferase deficiency states analyzed thus far. This may be explained in part by the more proximal position of ppGalNAcT-1 action in the pathway of core-type O glycosylation required for selectin ligand synthesis. While the formation of selectin ligands may continue in part among N-glycans (36), or perhaps via O glycosylation by other ppGalNAcT isozymes, core 1 and core 2 O-glycan branching cannot compensate in the absence of the ppGalNAcT-1-dependent linkage of GalNAc to serine or threonine.

The essential role of L-selectin ligands in lymphoid homing and lymph node homeostasis contrasts with findings regarding B-cell immune function. Selectin ligand expression does not correlate with Ig levels in circulation, nor does L-selectin deficiency dampen humoral immunity in assays of antigen-specific antibody production upon immunization. Humoral immune responses are, in fact, increased in the absence of L-selectin (49). These findings nevertheless imply that L-selectin likely has additional physiologic roles distinct from the effects of binding to its sLe^X glycan ligand. Our findings among ppGalNAcT-1-deficient mice revealed a significant humoral immune deficit that appeared to be independent of B-cell immune responses and altered leukocyte homing due to reduced L-selectin ligand levels. No alterations in B-cell immune responsiveness to LPS or IgM antigen receptor stimulation were observed in ppGalNAcT-1 deficiency, along with continued GC B-cell proliferation, and GC B-cell apoptosis was significantly increased. Moreover, B-cell trafficking and abundance in the spleen were normal, while reduced GCs associated with apoptotic B cells were nevertheless also observed in this tissue.

The abundance of circulating IgG was significantly reduced among ppGalNAcT-1-deficient mice, both prior to and subsequent to immunization with either T-cell-independent or T-cell-dependent antigens. This deficit did not extend to IgM or IgA, which were present at normal abundances. Centroblast and centrocyte apoptosis was elevated, with significantly decreased centrocyte numbers in ppGalNAcT-1-deficient GCs and a significant reduction of IgG expression and plasma B-cell abundance. Some IgG production continued and a reduced number of plasma cells remained, implicating a robust modulatory effect of ppGalNAcT-1 on this regulatory and differentiation process in the B-cell-mediated humoral immune response. ppGalNAcT-1 normally diminishes apoptotic signaling in GCs during the development of IgG-secreting plasma B cells. Yet levels of Fas at the B-cell surface were normal in ppGalNAcT-1 deficiency, and no alterations in the expression of other cell surface glycoproteins were as yet detected (data

not shown). Whether GC B-cell apoptosis in ppGalNAcT-1 deficiency is due to altered O glycosylation among B cells, dendritic cells, or possibly stromal cells that support the microenvironment is currently unknown. Such studies are necessary to ultimately identify the glycoprotein(s) involved and to further delineate the precise mechanisms by which ppGal NAcT-1-dependent protein O glycosylation modulates GC B-cell apoptosis and thereby the humoral immune response in vivo.

The initiation of protein O glycosylation in vivo by ppGal NAcT-1 translates into vital roles in vascular biology, hemostasis, and humoral immunity. Core-type protein O glycosylation is generally known to support mucin structure and function on endothelial cell surfaces, protecting cells against stress and pathogen infection (3, 51). Furthermore, it was recently shown that a loss of core 3 O-glycans in mice increases their susceptibility to colitis and colorectal tumors (1). Core-type O glycosylation is often produced following a stepwise and hierarchical pattern of peptide modification by multiple ppGal NAcT isozymes in generating a high-density array of O-glycans that assist in tissue hydration and can compete to block receptors carried by mucosal pathogens. Such physiologic roles, which have yet to be probed, may indeed be modulated by ppGalNAcT-1 and perhaps other ppGalNAcTs that normally act subsequently but fail to O glycosylate otherwise native glycopeptide sequences. Although ppGalNAcT-1 deficiency is likely compensated for to some degree in the intact mouse by other ppGalNAcT family members, the endogenous physiologic functions that we can now assign to ppGalNAcT-1 in blood coagulation, leukocyte trafficking, and humoral immunity are clearly dependent upon the substrate specificity and expression of this glycosyltransferase. The biologic activities of protein O glycosylation and the mechanisms by which this abundant posttranslational modification regulates cellular biology can be further resolved by experimental approaches that incorporate genetic, biochemical, and physiologic analyses of intact organisms.

ACKNOWLEDGMENTS

We thank Kurt Marek, James Yousif, and Yan Wang for expert assistance.

This research was partly funded by NIH grant DK48247 (J.D.M.) and by German Research Foundation grant AZ 428/2-1 (to A.Z.). J.D.M. is supported as an investigator of the Howard Hughes Medical Institute.

REFERENCES

1. **An, G., B. Wei, J. M. McDaniel, T. Ju, R. D. Cummings, J. Braun, and L. Xia.** 2007. Increased susceptibility to colitis and colorectal tumors in mice lacking core 3-derived O-glycans. J. Exp. Med. **204:**1417–1429.
2. **Arbones, M. L., D. C. Ord, K. Ley, H. Ratech, C. Maynard-Curry, G. Otten, D. J. Capon, and T. F. Tedder.** 1994. Lymphocyte homing and leukocyte rolling and migration are impaired in L-selectin-deficient mice. Immunity **1:**247–260.
3. **Bansil, R., E. Stanley, and J. T. LaMont.** 1995. Mucin biophysics. Annu. Rev. Physiol. **57:**635–657.
4. **Barbieri, A. M., M. Filopanti, G. Bua, and P. Beck-Peccoz.** 2007. Two novel nonsense mutations in GALNT3 gene are responsible for familial tumoral calcinosis. J. Hum. Genet. **52:**464–468.
5. **Bennet, E. P., H. Hassan, U. Mandel, E. Mirgorodskaya, P. Roepstorff, J. Burchell, J. Taylor-Papadimitriou, M. A. Hollingsworth, G. Merkx, A. Geurts van Kessel, H. Eiberg, R. Steffensen, and H. Clausen.** 1998. Cloning of a human UDP-*N*-acetyl-α-D-galactosamine:polypeptide *N*-acetylgalactosaminyltransferase that complements other GalNAc-transferases in complete O-glycosylation of the MUC1 tandem repeat. J. Biol. Chem. **273:**30472–30481.
6. **Berlin, C., E. L. Berg, M. J. Briskin, D. P. Andrew, P. J. Kilshaw, B. Holzmann, I. L. Weissman, A. Hamann, and E. C. Butcher.** 1993. Alpha 4 beta 7 integrin mediates lymphocyte binding to the mucosal vascular addressin MAdCAM-1. Cell **74:**185–195.
7. **Brockhausen, I., D. Toki, J. Brockhausen, S. Peters, T. Bielfeldt, A. Kleen, H. Paulsen, M. Meldal, F. Hagen, and L. A. Tabak.** 1996. Specificity of O-glycosylation by bovine colostrums UDP-GalNAc:polypeptide α-*N*-acetylgalactosaminyltransferase using synthetic glycopeptide substrates. Glycoconj. J. **13:**849–856.
8. **Brockhausen, I.** 2000. Biosynthesis of the O-glycan chains of mucins and mucin-type glycoproteins, p. 313–328. *In* B. Ernst, G. W. Hart, and P. Sinay (ed.), Carbohydrates in chemistry and biology, vol. 3. Wiley-VCH, New York, NY.
9. **Cheng, L., K. Tachibana, H. Iwasaki, A. Kameyama, Y. Zhang, T. Kubota, T. Hiruma, K. Tachibana, T. Kudo, J.-M. Guo, and H. Narimatsu.** 2004. Characterization of a novel human UDP-GalNAc transferase, ppGalNAc-T15. FEBS Lett. **566:**17–24.
10. **Elhammer, A., and S. Kornfeld.** 1986. Purification and characterization of UDP-*N*-acetylgalactosamine:polypeptide *N*-acetylgalactosaminyltransferase from bovine colostrum and murine lymphoma BW5147 cells. J. Biol. Chem. **261:**5249–5255.
11. **Ellies, L. G., S. Tsuboi, B. Petryniak, J. B. Lowe, M. Fukuda, and J. D. Marth.** 1998. Core 2 oligosaccharide biosynthesis distinguishes between selectin ligands essential for leukocyte homing and inflammation. Immunity **9:**881–890.
12. **Ellies, L. G., D. Ditto, G. G. Levy, M. Wahrenbrock, D. Ginsburg, A. Varki, D. Le, and J. D. Marth.** 2002. Sialyltransferase ST3Gal-IV operates as a dominant modifier of hemostasis by concealing asialoglycoprotein receptor ligands. Proc. Natl. Acad. Sci. USA **99:**10042–10047.
13. **Ellies, L. G., M. Sperandio, G. H. Underhill, J. Yousif, M. Smith, J. J. Priatel, G. S. Kansas, K. Ley, and J. D. Marth.** 2002. Sialyltransferase specificity in selectin ligand formation. Blood **100:**3618–3625.
14. **Fukuda, M., N. Hiraoka, T. O. Akama, and M. N. Fukuda.** 2001. Carbohydrate-modifying sulfotransferases: structure, function, and pathophysiology. J. Biol. Chem. **276:**47747–47750.
15. **Gauguet, J. M., S. D. Rosen, J. D. Marth, and U. H. von Andrian.** 2004. Core 2 branching beta1,6-*N*-acetylglucosaminyltransferase and high endothelial cell *N*-acetylglucosamine-6-sulfotransferase exert differential control over B- and T-lymphocyte homing to peripheral lymph nodes. Blood **104:**4104–4112.
16. **Gerken, T. A., C. Tep, and J. Rarick.** 2004. Role of peptide sequence and neighboring residue glycosylation on the substrate specificity of the uridine 5′-α-*N*-acetylgalactosamine:poly-peptide *N*-acetylgalactosaminyltransferases T1 and T2: kinetic modeling of the porcine and canine submaxillary gland mucin tandem repeats. Biochemistry **43:**9888–9900.
17. **Hagen, F. K., B. Van Wuyckhuyse, and L. A. Tabak.** 1993. Purification, cloning, and expression of a bovine UDP-GalNAc:polypeptide *N*-acetylgalactosaminyltransferase. J. Biol. Chem. **268:**18960–18965.
18. **Hagen, F. K., C. A. Gregoire, and L. A. Tabak.** 1995. Cloning and sequence homology of a rat UDP-GalNAc:polypeptide *N*-acetylgalactosaminyltransferase. Glycoconj. J. **12:**901–909.
19. **Hagen, F. K., K. G. Ten Hagen, T. M. Beres, M. Balys, B. C. Van Wuyckhuyse, and L. A. Tabak.** 1997. cDNA cloning and expression of a novel UDP-GalNAc:polypeptide *N*-acetylgalactosaminyltransferase. J. Biol. Chem. **272:**13843–13848.
20. **Hanisch, F.-G., S. Muller, H. Hassan, H. Clausen, N. Zachara, A. A. Gooley, H. Paulsen, K. Alving, and J. Peter-Katalinic.** 1999. Dynamic epigenetic regulation of initial O-glycosylation by UDP-*N*-acetylgalactosamine:peptide *N*-acetylgalactosaminyltransferases. J. Biol. Chem. **274:**9946–9954.
21. **Hemmerich, S., A. Bistrup, M. S. Singer, A. van Zante, J. K. Lee, D. Tsay, M. Peters, J. L. Carminati, T. J. Brennan, K. Carver-Moore, et al.** 2001. Sulfation of L-selectin ligands by an HEV-restricted sulfotransferase regulates lymphocyte homing to lymph nodes. Immunity **15:**237–247.
22. **Hennet, T., F. K. Hagen, L. A. Tabak, and J. D. Marth.** 1995. T-cell-specific deletion of a polypeptide *N*-acetylgalactosaminyl-transferase gene by site-directed recombination. Proc. Natl. Acad. Sci. USA **92:**12070–12074.
23. **Hiraoka, N., H. Kawashima, B. Petryniak, J. Nakayama, J. Mitoma, J. D. Marth, J. B. Lowe, and M. Fukuda.** 2004. Core 2 branching beta1,6-*N*-acetylglucosaminyltransferase and high endothelial venule-restricted sulfotransferase collaboratively control lymphocyte homing. J. Biol. Chem. **279:**3058–3067.
24. **Homa, F. L., T. Hollander, D. J. Lehman, D. R. Thomsen, and A. P. Elhammer.** 1993. Isolation and expression of a cDNA clone encoding a bovine UDP-GalNAc:polypeptide *N*-acetylgalactosaminyltransferase. J. Biol. Chem. **268:**12609–12616.
25. **Homeister, J. W., A. D. Thall, B. Petryniak, P. Maly, C. E. Rogers, P. L. Smith, R. J. Kelly, K. M. Gersten, S. W. Askari, G. Cheng, et al.** 2001. The alpha(1,3)fucosyltransferases FucT-IV and FucT-VII exert collaborative control over selectin-dependent leukocyte recruitment and lymphocyte homing. Immunity **15:**115–126.
26. **Ichikawa, S., K. W. Lyles, and M. J. Econs.** 2005. A novel *GALNT3* mutation in a pseudoautosomal dominant form of tumoral calcinosis: evidence that

the disorder is autosomal recessive. J. Clin. Endocrinol. Metab. **90:**2420–2423.
27. **Ju, T., and R. D. Cummings.** 2005. Protein glycosylation: chaperone mutation in Tn syndrome. Nature **437:**1252.
28. **Kato, K., H. Takeuchi, N. Miyahara, A. Kanoh, H. Hassan, H. Clausen, and T. Irimura.** 2001. Distinct order of GalNAc incorporation into a peptide with consecutive threonines. Biochem. Biophys. Res. Commun. **287:**110–115.
29. **Kato, K., C. Jeanneau, M. A. Tarp, A. Benet-Pages, B. Lorenz-Depiereux, E. P. Bennett, U. Mandel, T. M. Strom, and H. Clausen.** 2006. Polypeptide GalNAc-transferase T3 and familial tumoral calcinosis. Secretion of fibroblast growth factor 23 requires O-glycosylation. J. Biol. Chem. **281:**18370–18377.
30. **Kingsley, P. D., K. G. Ten Hagen, K. M. Maltby, J. Zara, and L. A. Tabak.** 2000. Diverse spatial expression patterns of UDP-GalNAc:polypeptide N-acetylgalactosaminyltransferase family member mRNAs during mouse development. Glycobiology **10:**1317–1323.
31. **Kraal, G., I. L. Weissman, and E. C. Butcher.** 1982. Germinal centre B cells: antigen specificity and changes in heavy chain class expression. Nature **298:**377–379.
32. **Lowe, J. B., and J. D. Marth.** 2003. A genetic approach to mammalian glycan function. Annu. Rev. Biochem. **72:**643–691.
33. **Maly, P., A. Thall, B. Petryniak, C. E. Rogers, P. L. Smith, R. M. Marks, R. J. Kelly, K. M. Gersten, G. Cheng, T. L. Saunders, et al.** 1996. The alpha(1,3)fucosyltransferase Fuc-TVII controls leukocyte trafficking through an essential role in L-, E-, and P-selectin ligand biosynthesis. Cell **86:**643–653.
34. **Marth, J. D.** 1996. Complexity in O-linked oligosaccharide biosynthesis engendered by multiple polypeptide *N*-acetylgalactosaminyltransferases. Glycobiology **6:**701–705.
35. **McGuire, E. J., and S. Roseman.** 1967. Enzymatic synthesis of the protein-hexosamine linkage in sheep submaxillary mucin. J. Biol. Chem. **242:**3745–3755.
36. **Mitoma, J., X. Bao, B. Petryniak, P. Schaerli, J. M. Gauguet, S. Y. Yu, H. Kawashima, H. Saito, K. Ohtsubo, J. D. Marth, K. H. Khoo, U. H. von Andrian, J. B. Lowe, and M. Fukuda.** 2007. Critical functions of N-glycans in L-selectin-mediated lymphocyte homing and recruitment. Nat. Immunol. **8:**409–418.
37. **Nehrke, K., F. K. Hagen, and L. A. Tabak.** 1998. Isoform-specific O-glycosylation by murine UDP-GalNAc:polypeptide *N*-acetylgalactosaminyltransferase-T3, in vivo. Glycobiology **8:**367–371.
38. **Ohtsubo, K., and J. D. Marth.** 2006. Glycosylation in cellular mechanisms of health and disease. Cell **126:**855–867.
39. **Piccio, L., B. Rossi, L. Colantonio, R. Grenningloh, A. Gho, L. Ottoboni, J. W. Homeister, E. Scarpini, M. Martinello, C. Laudanna, D. D'Ambrosio, J. B. Lowe, and G. Constantin.** 2005. Efficient recruitment of lymphocytes in inflamed brain venules requires expression of cutaneous lymphocyte antigen and fucosyltransferase-VII. J. Immunol. **174:**5805–5813.
40. **Pratt, M. R., H. C. Hang, K. G. Ten Hagen, J. Rarick, T. A. Gerken, L. A. Tabak, and C. R. Bertozzi.** 2004. Deconvoluting the functions of polypeptide N-alpha-acetylgalactosaminyltransferase family members by glycopeptide substrate profiling. Chem. Biol. **11:**1009–1016.
41. **Priatel, J. J., M. Sarkar, H. Schachter, and J. D. Marth.** 1997. Isolation, characterization and inactivation of the mouse *Mgat3* gene: the bisecting N-acetylglucosamine in asparagine-linked oligosaccharides appears dispensable for viability and reproduction. Glycobiology **7:**45–56.
42. **Priatel, J. J., D. Chui, N. Hiraoka, C. T. Simmons, K. B. Richardson, D. M. Page, M. Fukuda, N. Varki, and J. D. Marth.** 2000. The ST3Gal-I sialyltransferase controls CD8+ T cell homeostasis by modulating O-glycan biosynthesis. Immunity **12:**273–283.
43. **Rosen, S. D.** 2004. Ligands for L-selectin: homing, inflammation, and beyond. Annu. Rev. Immunol. **22:**129–156.
44. **Sastry, M. V., P. Banarjee, S. R. Patanjali, M. J. Swamy, G. V. Swarnalatha, and A. Surolia.** 1986. Analysis of saccharide binding to Artocarpus integrifolia lectin reveals specific recognition of T-antigen (beta-D-Gal(1-3)D-GalNAc). J. Biol. Chem. **261:**11726–11733.
45. **Schachter, H., and I. Brockhausen.** 1989. The biosynthesis of branched O-glycans. Symp. Soc. Exp. Biol. **43:**1–26.
46. **Schwientek, T., E. P. Bennett, C. Flores, J. Thacker, M. Hollmann, C. A. Reis, J. Behrens, U. Mandel, B. Keck, M. A. Schafer, et al.** 2002. Functional conservation of subfamilies of putative UDP-*N*-acetylgalactosamine:polypeptide *N*-acetylgalactosaminyltransferases in Drosophila, Caenorhabditis elegans, and mammals. One subfamily composed of l(2)35Aa is essential in Drosophila. J. Biol. Chem. **277:**22623–22638.
47. **Shafi, R., S. P. Iyer, L. G. Ellies, N. O'Donnell, K. W. Marek, D. Chui, G. W. Hart, and J. D. Marth.** 2000. The O-GlcNAc transferase gene resides on the X chromosome and is essential for embryonic stem cell viability and mouse ontogeny. Proc. Natl. Acad. Sci. USA **97:**5735–5739.
48. **Sorensen, T., T. White, H. H. Wandall, A. K. Kristensen, P. Roepstorff, and H. Clausen.** 1995. UDP-*N*-acetyl-α-D-galactosamine:polypeptide *N*-acetylgalactosaminyltransferase: identification and separation of two distinct transferase activities. J. Biol. Chem. **270:**24166–24173.
49. **Steeber, D. A., N. E. Green, S. Sato, and T. F. Tedder.** 1996. Humoral immune responses in L-selectin-deficient mice. J. Immunol. **157:**4899–4907.
50. **Stevens, S. K., I. L. Weissman, and E. C. Butcher.** 1982. Differences in the migration of B and T lymphocytes: organ-selective localization in vivo and the role of lymphocyte-endothelial cell recognition. J. Immunol. **2:**844–851.
51. **Tabak, L. A.** 1995. In defense of the oral cavity: structure, biosynthesis, and function of salivary mucins. Annu. Rev. Physiol. **57:**547–564.
52. **Tang, M. L., D. A. Steeber, X. Q. Zhang, and T. F. Tedder.** 1998. Intrinsic differences in L-selectin expression levels affect T and B lymphocyte subset-specific recirculation pathways. J. Immunol. **160:**5113–5121.
53. **Ten Hagen, K. G., D. Tetaert, F. K. Hagen, C. Richet, T. M. Beres, J. Gagnon, M. M. Balys, B. VanWuyckhuyse, G. S. Bedi, P. Degand, and L. A. Tabak.** 1999. Characterization of a UDP-GalNAc:polypeptide *N*-acetylgalactosaminyltransferase which displays glycopeptide *N*-acetylgalactosaminyltransferase activity. J. Biol. Chem. **274:**27867–27874.
54. **Ten Hagen, K. G., and D. T. Tran.** 2002. A UDP-GalNAc:polypeptide *N*-acetylgalactosaminyltransferase is essential for viability in *Drosophila melanogaster*. J. Biol. Chem. **277:**22616–22622.
55. **Ten Hagen, K. G., T. A. Fritz, and L. A. Tabak.** 2003. All in the family: the UDP-GalNAc:polypeptide *N*-acetylgalactosaminyltransferases. Glycobiology **13:**1R–16R.
56. **Tian, E., and K. G. Ten Hagen.** 2007. A UDP-GalNAc:polypeptide *N*-acetylgalactosaminyltransferase is required for epithelial tube formation. J. Biol. Chem. **282:**606–614.
57. **Topaz, O., D. L. Shurman, R. Bergman, M. Indelman, P. Ratajczak, M. Mizrachi, Z. Khamaysi, D. Behar, D. Petronius, V. Friedman, I. Zelikovic, S. Raimer, A. Metzker, G. Richard, and E. Sprecher.** 2004. Mutations in *GALNT3*, encoding a protein involved in O-linked glycosylation, cause of familial tumoral calcinosis. Nat. Genet. **36:**579–581.
58. **Van den Steen, P., P. M. Rudd, R. A. Dwek, and G. Opdenakker.** 1998. Concepts and principles of O-linked glycosylation. Crit. Rev. Biochem. Mol. Biol. **33:**151–208.
59. **Van Dyken, S. J., R. S. Green, and J. D. Marth.** 2007. Structural and mechanistic features of protein O glycosylation linked to $CD8^+$ T-cell apoptosis. Mol. Cell. Biol. **27:**1096–1111.
60. **Wandall, H. H., H. Hassan, E. Mirgorodskaya, A. K. Kristensen, P. Roepstorff, E. P. Bennett, P. A. Nielsen, M. A. Hollingsworth, J. Burchell, J. Taylor-Papadimitriou, and H. Clausen.** 1997. Substrate specificities of three members of the human UDP-*N*-acetyl-α-D-galactosamine:polypeptide *N*-acetylgalactosaminyltransferase family, GalNAc-T1, -T2, and -T3. J. Biol. Chem. **272:**23503–23514.
61. **Wang, Y., J. L. Abernathy, A. E. Eckhardt, and R. L. Hill.** 1992. The acceptor substrate specificity of porcine submaxillary UDP-GalNAc:polypeptide *N*-acetylgalactosaminyltransferase is dependent on the amino acid sequences adjacent to serine and threonine residues. J. Biol. Chem. **267:**12709–12716.
62. **Wang, Y., J. Tan, M. Sutton-Smith, D. Ditto, M. Panico, R. M. Campbell, N. M. Varki, J. M. Long, J. Jaeken, S. R. Levinson, A. Wynshaw-Boris, H. R. Morris, D. Le, A. Dell, H. Schachter, and J. D. Marth.** 2001. Modeling human congenital disorder of glycosylation type IIa in the mouse: conservation of asparagine-linked glycan-dependent functions in mammalian physiology and insights into disease pathogenesis. Glycobiology **11:**1–20.
63. **White, T., E. P. Bennett, K. Takio, T. Sorensen, N. Bonding, and H. Clausen.** 1995. Purification and cDNA cloning of a human UDP-*N*-acetyl-α-D-galactosamine:polypeptide *N*-acetylgalactosaminyltransferase. J. Biol. Chem. **270:**24156–24165.
64. **Xiao, Y., J. Hendriks, P. Langerak, H. Jacobs, and J. Borst.** 2004. CD27 is acquired by primed B cells at the centroblast stage and promotes germinal center formation. J. Immunol. **172:**7432–7441.
65. **Yeh, J. C., N. Hiraoka, B. Petryniak, J. Nakayama, L. G. Ellies, D. Rabuka, O. Hindsgaul, J. D. Marth, J. B. Lowe, and M. Fukuda.** 2001. Novel sulfated lymphocyte homing receptors and their control by a Core1 extension beta 1,3-*N*-acetylglucosaminyltransferase. Cell **105:**957–969.
66. **Young, W. W., D. R. Holcomb, K. G. Ten Hagen, and L. A. Tabak.** 2003. Expression of UDP-GalNAc:polypeptide *N*-acetylgalactosaminyltransferase isoforms in murine tissues determined by real-time PCR: a new view of a large family. Glycobiology **13:**549–557.
67. **Zarbock, A., C. A. Lowell, and K. Ley.** 2007. Spleen tyrosine kinase Syk is necessary for E-selectin-induced αLβ2 integrin-mediated rolling on intercellular adhesion molecule-1. Immunity **26:**773–783.
68. **Zhang, Y., H. Iwasaki, H. Wang, T. Kudo, T. B. Kalka, T. Hennet, T. Kubota, L. Cheng, N. Inaba, M. Gotoh, et al.** 2003. Cloning and characterization of a new human UDP-*N*-acetyl-alpha-D-galactosamine:polypeptide *N*-acetylgalactosaminyltransferase, designated pp-GalNAc-T13, that is specifically expressed in neurons and synthesizes GalNAc alpha-serine/threonine antigen. J. Biol. Chem. **278:**573–584.